NANO LETTERS

2005
Vol. 5, No. 11
2135−2138

Achieving High-Current Carbon Nanotube Emitters

Eric Minoux,*,† Oliver Groening,‡ Kenneth B. K. Teo,§ Sharvari H. Dalal,§ Laurent Gangloff,§ Jean-Philippe Schnell,† Ludovic Hudanski,† Ian Y. Y. Bu,§ Pascal Vincent,† Pierre Legagneux,† Gehan A. J. Amaratunga,§ and William I. Milne§

Thales Research & Technology, Route départementale 128, 91 767 Palaiseau Cedex, France, EMPA Materials Science and Technology, Feuerwerkerstrasse 39, Thun CH 3602, Switzerland, and Engineering Department, University of Cambridge, Trumpington Street, Cambridge CB2 1PZ, United Kingdom

Received July 20, 2005; Revised Manuscript Received August 26, 2005

ABSTRACT

When a carbon nanotube emitter is operated at high currents (typically above 1 μA per emitter), a small voltage drop (∼few volts) along its length or at its contact generates a reverse/canceling electric field that causes a saturation-like deviation from the classical Fowler–Nordheim behavior with respect to the applied electric field. We present a correction to the Fowler–Nordheim equation to account for this effect, which is experimentally verified using field emission and contact electrical measurements on individual carbon nanotube emitters. By using rapid thermal annealing to improve both the crystallinity of the carbon nanotubes and their electrical contact to the substrate, it is possible to reduce this voltage drop, allowing very high currents of up to 100 μA to be achieved per emitter with no significant deviation from the classical Fowler–Nordheim behavior.

Carbon nanotubes/nanofibers (CNs) are currently studied as field emission electron sources for use in a variety of applications such as microwave amplifiers,[1] electron guns,[2] X-ray sources,[3] parallel electron beam lithography,[4] and flat panel displays.[5] Whiskerlike in shape and high in aspect ratio, carbon nanotubes present the ideal shape for field emission[6] (FE), with enhancement factors in the range of 100−1000. Because of strong C−C covalent bonds, CNs are much less sensitive to electromigration than metallic tips or filaments and are thus able to carry high current densities,[7,8] ranging from 10^7 to 10^9 A cm^{-2}. CNs are also unique in that they can field emit very stable currents even when self-heating of the emitter increases the temperature of the apex up to 2000 K.[9]

Although an individual CN emitter can be operated at currents above 10 μA,[10] most FE applications require significantly higher currents (10−100 mA), and thus, cathodes comprising a large number of CNs are required. The ideal field emitter array would be an ordered array of individual, vertically aligned emitters spaced by approximately twice their height in order to minimize field screening while keeping high emitter density.[11] Plasma-enhanced chemical vapor deposition (PECVD) offers a well-controlled technique for the production of such vertically aligned multiwall CN arrays with industrial fabrication potential. By using this technique, we have grown arrays of well-spaced individual CN emitters and tested their FE properties.[12] At present, the currents for as-grown CNs are lower than required for certain applications because of the high density of defects in PECVD CNs. In this article, we show that rapid thermal annealing (RTA) in the 800 °C range allows more than 1 order of magnitude higher currents and appreciably improves crystal structure.

An array of individual CNs was prepared by dc PECVD of acetylene and ammonia at 700 °C.[13] The growth of individual CNs was achieved by using 100-nm-diameter patterned dots of 7-nm-thick Ni catalyst on a 8-nm-thick TiN diffusion barrier on a highly conductive n^+ doped Si substrate. This process delivers highly uniform CNs with mean radius $r \sim 25$ nm and height $h \sim 5$ μm for 45 min of growth time (see Figure 1a). Typically, the standard deviation in the radius and height distributions of the CNs is 4.1 and 6.3%, respectively,[14] so that the aspect ratio (h/r) of most of the nanotubes in the array is around 200.

FE measurements were performed on individual CNs using a high-resolution scanning anode field emission microscope[15] (SAFEM) (see Figure 1b). The SAFEM tip radius was 1 μm and the tip-to-CN apex distance was typically ∼10−15 μm. The pitch of the array was 50 μm to avoid measurement of

* Corresponding author. E-mail: eric.minoux@thalesgroup.com.
† Thales Research & Technology.
‡ Federal Laboratories for Materials Testing and Research.
§ Engineering Department, University of Cambridge.

10.1021/nl051397d CCC: $30.25
Published on Web 10/25/2005

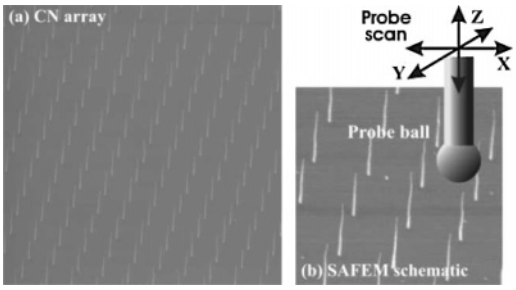

Figure 1. (a) Uniform array of individual vertically aligned CNs grown by dc PECVD at 700 °C. In this micrograph, the CNs are 5 μm in length, 50 nm in diameter, and the spacing is 5 μm. (b) Schematic of the scanning anode field emission microscope (SAFEM).

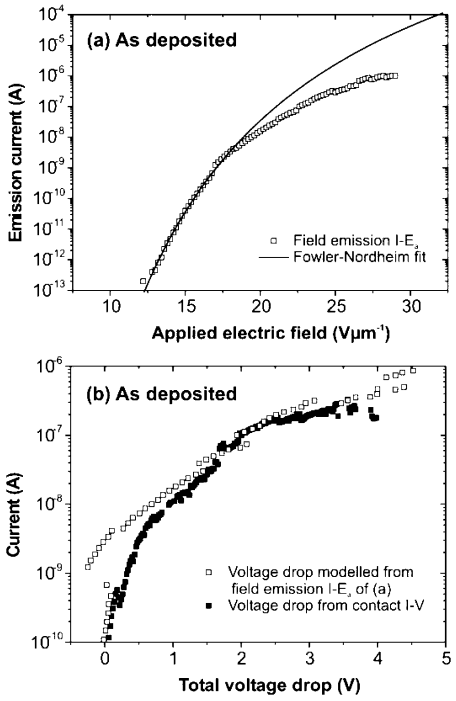

Figure 2. (a) Field emission $I-E_a$ characteristic obtained from an as-deposited CN. The line corresponds to the fit to the FN model at low currents. (b) Measured (by touching the probe with the CN) and calculated (from field emission $I-E_a$ characteristic with $\alpha = 1$) voltage drops for the same as-deposited CN.

adjacent CNs. Stable and reproducible characteristics were obtained by cycling the current-applied electric field ($I-E_a$) characteristics to 1 μA, as described by Semet.[16]

At low applied fields and currents, the $I-E_a$ behavior of as-deposited CNs follows closely the Fowler−Nordheim (FN) equation (with image charge correction) (see Figure 2a) written as:[17]

$$I(E_a) = A\frac{1.42 \times 10^{-6}}{\Phi}(\beta E_a)^2 \exp\left(\frac{10.4}{\sqrt{\Phi}}\right)\exp\left(-\frac{6.56 \times 10^9 \Phi^{1.5}}{\beta E_a}\right) \quad (1)$$

where I is the emission current (A), A the emission area (m^2), E_a the applied electric field (V m^{-1}), Φ the work function (eV), and β the electric field enhancement factor. In this low-current regime, assuming a work function of 4.9 eV,[18,19] the derived field enhancement factor of 190 is in good agreement with the aspect ratio of CNs as measured by SEM.

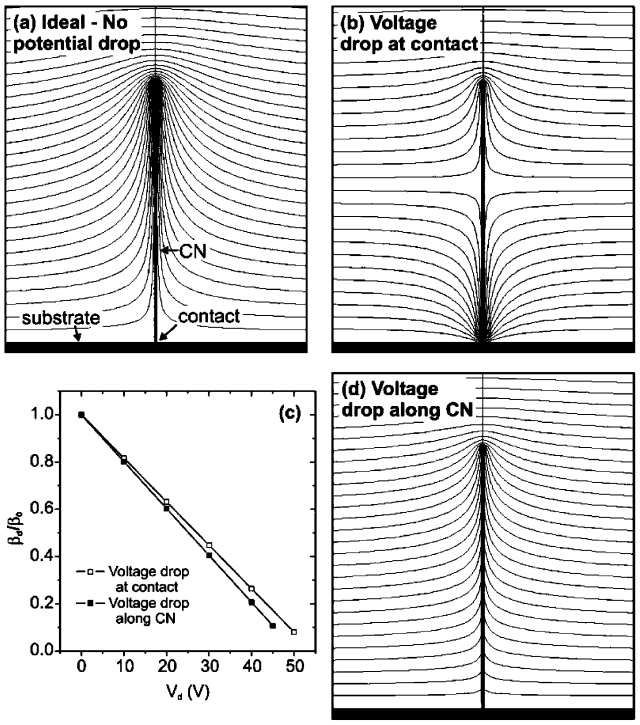

Figure 3. Simulations show the distribution of equipotential lines between the CN and the anode: (a) depicts the case of a perfect emitter where there is no potential drop along it, (b) an emitter with a voltage drop at the emitter/substrate interface, and (d) an emitter with a voltage drop along its length. The graph in (c) plots the reduction of field enhancement factor as a function of the voltage drop. In this particular case, the emitter height was 5 μm, its radius was 25 nm, and the applied electric field was 10 V μm^{-1}.

However, typically at currents above 1 μA, a strong saturation of the emitted current is observed and the curves deviate significantly from FN law (see Figure 2a). Two explanations for this observation have been proposed in the literature: (a) the presence of adsorbates (adsorbed molecules or impurities) at the CN apex can enhance field emission at low fields, which are then removed at high fields, causing the current to saturate,[16,19] or (b) the presence of a resistance *in series* with the emitter, for example a bad CN/substrate electrical contact, can induce a saturation at high applied fields,[20] Here, we demonstrate both experimentally and through simulations that the emitter current saturation is due to a large voltage drop along the CN emitter and/or at the CN/substrate interface.

A voltage drop may appear at two places: (1) along the CN or (2) at the CN/substrate interface. To study the effect of both these voltage drops on the emitter field enhancement factor, the distribution of electrostatic potentials between a CN and an anode for 3 different configurations has been simulated using CPO 3D software.[21] First, the case where no potential drop exists in the system is presented in Figure 3a. In this case, the CN has a field enhancement factor of β_0. Next, a potential difference, V_d, is introduced at the CN/substrate contact. From Figure 3b, one can see that only

equipotentials above V_d run around the CN's apex. This situation is equivalent to a reduced apparent effective length of CN, resulting in a lower field enhancement factor β_d. We determined β_d for various V_d, and we obtained a linear dependence of β_d/β_0 versus V_d (see Figure 3c). By studying various CN geometries, the following relationship has been deduced:

$$\frac{\beta_d}{\beta_0} = 1 - \alpha\frac{V_d}{hE_a} \qquad (2)$$

with h the emitter height (m), E_a the applied electric field (Vm^{-1}), and α, which is equal to 0.92. Last, we assume that the voltage drop is generated along the CN's length (see Figure 3d) rather than just at the contact. The same relationship is found to apply except with α equal to 1. Hence, a voltage drop occurring at the CN/substrate interface or along the CN length has, in practical terms, almost the same effect on the $I-E_a$ characteristics.

The β in the FN eq 1 can now be replaced by β_d of eq 2 to accurately model emitter voltage losses during FE. Using the experimental data of Figure 2a and a β_0 of 190 deduced from the FN fit at low voltages, we have calculated that V_d ranges from 0 to 7.1 V (for $\alpha = 0.92$, i.e., contact effect) or from 0 to 6.5 V (for $\alpha = 1$, i.e., CN's resistive effect) when I varied from 10^{-10} to 10^{-6} A (see Figure 2b). To verify the validity of our formula, the SAFEM tip is now brought in contact with this CN to measure its actual $I-V$ characteristic. Figure 2b shows that, indeed, the contact $I-V$ measurements are a good fit to the $I-V_d$ deduced from the FE measurements. Thus, this experiment proves the validity of our model in which the enhancement factor is a function of the emitter voltage drop.

Note that this effect is prominent here because the CN voltage drop (a few volts at μA) along the CN length (a few microns) now generates a "canceling" electric field of the same order of magnitude of the applied field (a few volts/micron).

From the contact $I-V$, it is deduced that the total resistance between the substrate and the CN apex is on the order of $\sim$100 MΩ at 1 V, and thus, the conductivity is around 0.3 Ω^{-1} cm^{-1}. If we assume that the as-grown CNs were well crystallized, they should exhibit a conductivity value close to graphite (10^4 $\Omega^{-1}cm^{-1}$) and possess a resistance $\sim$3 kΩ. This small resistance would generate insignificant voltage drops ($\sim$mV) for currents in the μA range, which implies that most of the voltage drop is occurring at the CN/substrate interface. However, such large voltage drops ($\sim$7 V) are unlikely to exist only at the thin interface between the 8 nm TiN film and the CN. Thus, we believe that the voltage drop occurs along the CN in this case. The development of a voltage drop may also lead to heating effects that determine the maximum current a CN can support.[9,22]

To improve the emission behavior of the as-grown CNs, rapid thermal annealing in high vacuum (10^{-6} mbar) at high temperature (850 °C) was performed, followed by SAFEM measurements. Several nanotubes were measured, and the field enhancement factors were virtually the same before and after annealing in the low-current range (<0.1 μA). However, as seen in Figure 4a, no saturation was observed until a current of $\sim$20 μA. The field-emitted current now follows the FN characteristic over 8 orders of magnitude. The contact $I-V$ measurements on the postannealed CN (see Figure 4b) reveal that, at the same applied voltages, the postannealed CN has current approximately 3 orders of magnitude larger than that of the as-grown CN. By using the experimental data and the modified formula of the enhancement factor β_d, V_d have been determined for I from 10^{-8} to 5×10^{-5} A, and these are well correlated with the contact measurements (see Figure 4b). The resistance between the substrate and the CN apex is on the order of 100 kΩ at 1 V, and thus, the conductivity is around 3×10^2 $\Omega^{-1}cm^{-1}$. The maximum FE current supported by the postannealed CN before failure was between 80 and 120 μA (tens of CNs tested). This corresponds to a current density of $\sim 5 \times 10^6$ A cm^{-2} within one CN (CN diameter is 50 nm).

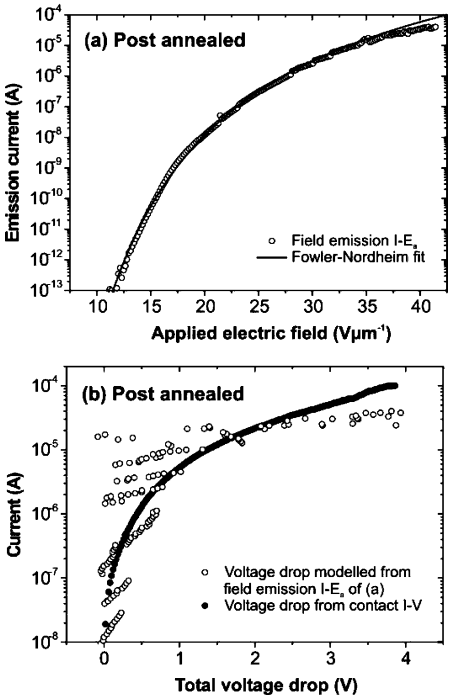

Figure 4. (a) $I-E_a$ characteristics obtained on a postannealed CN. The line corresponds to the best fit to the FN model. (b) Measured (by touching the probe with the CN) and calculated (from field emission $I-E_a$ characteristics with $\alpha = 1$) voltage drops for the same postannealed CN.

Further investigations were carried out to determine the extent of CN structure improvement due to RTA. Figure 5a and b show the CN apexes by using transmission electron microscopy. In our growth process, the Ni catalyst particle is always located at the CN apex (tip growth mechanism), with a thin carbon layer encapsulating it. For as-grown CNs, this layer is highly disordered (see Figure 5a). In contrast, after 850 °C annealing, well-crystallized graphene layers now cover the Ni catalyst at the CN apex (see Figure 5b). Postannealed CNs also exhibit relatively well-graphitized walls compared to those of as-grown CNs (see Figure 5c and d). The vibrational properties of as-grown CNs and postannealed CNs were also investigated by using Raman

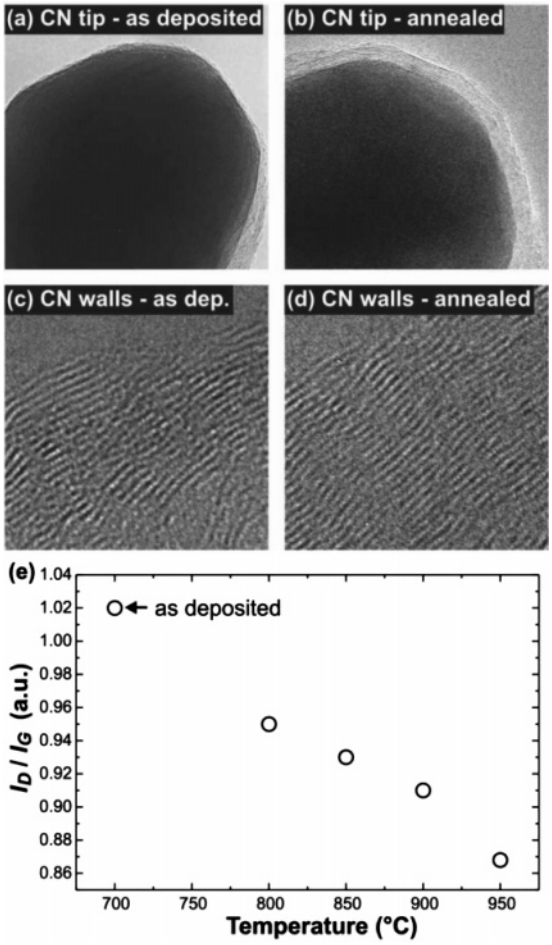

Figure 5. Transmission electron microscopy images of (a) as-grown and (b) postannealed CN's apex, and (c) as-grown and (d) postannealed CN's walls (in these cases, rapid thermal annealing was performed at 850 °C). (e) Variation of Raman I_D/I_G ratio versus annealing temperature.

spectroscopy. To qualitatively evaluate the crystalline structure, the ratio I_D/I_G between the two first-order peaks of graphite was determined as a function of annealing temperature. Crystalline graphite leads to a vibration mode at 1580 cm^{-1} named G (the graphite mode) peak. The peak at 1355 cm^{-1} is considered to represent a more disordered structure and is labeled D (the defect mode) peak. This ratio decreases with increasing annealing temperature (see Figure 5e), indicating a reducing fraction of defects found in the annealed CN. It is also known that structural imperfections will broaden these first-order Raman peaks. From as-grown CNs to postannealed CNs at 950 °C, we observed that the full width half-maximum (fwhm) of the G band decreased from 110 to 100 cm^{-1}, and that of the D band from 252 to 226 cm^{-1}, providing further evidence that improvement of the structure was occurring with increasing annealing temperature. This improvement of CN crystallinity is attributed to the carbonization process that occurs between 800 and 1500 °C[23] and which in turn can drastically diminish the electrical resistivity.

Moreover, we also propose that annealing improves the electrical contact between CN and the TiN diffusion barrier. It has been reported that carbide formation between carbon nanotubes and Ti occurs at temperatures above 800 °C and this leads to lower resistance contacts.[24,25]

In conclusion, a voltage drop of merely a few volts along an emitter can cause the emission current of the emitter to saturate. This effect is prominent here because the CN voltage drop (a few volts at μA) along the CN length (a few microns) generates a "canceling" electric field in the same magnitude of the applied field (a few volts/micron). By using simulation, a new formula has been derived to determine the field enhancement factor as a function of this voltage drop. The validity of this formula was verified by using both field emission and contact measurements on individual field emitters. Through rapid thermal annealing at 850 °C, the crystallinity of PECVD carbon nanotubes is improved. This posttreatment enables the production of arrays of CN emitters, each capable of 80−120 μA emission current. Such an array has been fabricated (CN density of 10^6 cm^{-1}) and delivers 30 mA peak current (12 A cm^{-2}) when directly modulated at microwave frequency (1.5 GHz).[26] This opens numerous new possibilities in high-current applications.

Acknowledgment. This work was funded by the European Commission through the IST-FET project CANVAD. K. B. K. Teo acknowledges the support of the Royal Academy of Engineering and Christ's College Cambridge.

References

(1) Read, M. E.; In Proceedings of the 2001 Particle Accelerator Conference, Chicago, **2001**, **2**, 1026.
(2) de Jonge, N.; *Nature (London)* **2002**, *420*, 393.
(3) Cheng, Y.; *Rev. Sci. Instrum.* **2004**, *75*, 3264.
(4) Teo, K. B. K.; *J. Vac. Sci. Technol., B* **2003**, *21*, 693.
(5) Chung, D.-S.; *Appl. Phys. Lett.* **2002**, *80*, 4045.
(6) Utsumi, T.; *IEEE Trans. Electron. Devices* **1991**, *38*, 2276.
(7) Franck, S.; *Science* **1998**, *280*, 1744.
(8) Lee, S.-B.; *J. Vac. Sci. Technol., B* **2002**, *20*, 2773.
(9) Purcell, S. T.; *Phys. Rev. Lett.* **2002**, *88*, 105502.
(10) de Jonge, N.; *Ultramicroscopy* **2003**, *95*, 85.
(11) Groening, O.; *J. Vac. Sci. Technol., B* **2000**, *18*, 665.
(12) Milne, W. I.; *Diamond Relat. Mater*. **2003**, *12*, 422.
(13) Chhowalla, M.; *J. Appl. Phys*. **2001**, *90*, 5308.
(14) Teo, K. B. K.; *Nanotechnology* **2003**, *14*, 204.
(15) Nilsson, L.; *J. Vac. Sci. Technol., B* **2000**, *20*, 326.
(16) Semet, V.; *Appl. Phys. Lett.* **2002**, *81*, 343.
(17) Brodie, I.; Spindt, C. *Adv. Electron. Electron Phys.* **1992**, *83*, 1.
(18) de Jonge, N.; *Appl. Phys. Lett*. **2004**, *85*, 1607.
(19) Dean, K. A.; *Appl. Phys. Lett.* **2000**, *76*, 375.
(20) Bonard, J.-M.; *Phys. Rev. B* **2003**, *67*, 115406.
(21) Charged Particle Optics Programs, CPO Ltd, Registered Company Number 4012016, Manchester, UK.
(22) Vincent, P.; *Phys. Rev. B* **2002**, *66*, 075406.
(23) Goma, J.; *Thin Solid Films* **1980**, *65*, 221.
(24) Zhang, Y.; *Science* **1999**, *285*, 1719.
(25) Martel, R.; *Phys. Rev. Lett.* **2001**, *87*, 256805.
(26) Teo, K. B. K. *Nature* **2005**, *437*, 968..

NL051397D